A combinatorial TIR1/AFB–Aux/IAA co-receptor system for differential sensing of auxin

Luz Irina A Calderón Villalobos[1,2,10], Sarah Lee[3], Cesar De Oliveira[4], Anthony Ivetac[4], Wolfgang Brandt[5], Lynne Armitage[6], Laura B Sheard[7,8,11], Xu Tan[7,8,10], Geraint Parry[1,2,9], Haibin Mao[7,8], Ning Zheng[7,8], Richard Napier[3], Stefan Kepinski[6] & Mark Estelle[1,2]*

The plant hormone auxin regulates virtually every aspect of plant growth and development. Auxin acts by binding the F-box protein TRANSPORT INHIBITOR RESPONSE 1 (TIR1) and promotes the degradation of the AUXIN/INDOLE-3-ACETIC ACID (Aux/IAA) transcriptional repressors. Here we show that efficient auxin binding requires assembly of an auxin co-receptor complex consisting of TIR1 and an Aux/IAA protein. Heterologous experiments in yeast and quantitative IAA binding assays using purified proteins showed that different combinations of TIR1 and Aux/IAA proteins form co-receptor complexes with a wide range of auxin-binding affinities. Auxin affinity seems to be largely determined by the Aux/IAA. As there are 6 TIR1/AUXIN SIGNALING F-BOX proteins (AFBs) and 29 Aux/IAA proteins in *Arabidopsis thaliana*, combinatorial interactions may result in many co-receptors with distinct auxin-sensing properties. We also demonstrate that the AFB5–Aux/IAA co-receptor selectively binds the auxinic herbicide picloram. This co-receptor system broadens the effective concentration range of the hormone and may contribute to the complexity of auxin response.

AA (**1**) is a small tryptophan-derived phytohormone that regulates many plant growth and developmental processes[1] including embryogenesis[2,3], tropic growth[4], leaf formation[5], stem elongation[6], root elongation[7] and fruit development[8]. A number of synthetic auxinic compounds have also been identified, most notably 1-naphthaleneacetic acid (1-NAA, **2**) and the widely used herbicides 2,4-dichlorophenoxyacetic acid (2,4-D, **3**) and picolinate derivatives instanced by 4-amino-3,5,6-trichloro-2-pyridinecarboxylic acid (picloram, **4**)[9]. Recent studies have produced a coherent model for auxin perception and transcriptional regulation. At low auxin levels, Aux/IAA transcriptional repressors[10–12], together with co-repressor proteins including TOPLESS[13,14], repress genes targeted by auxin response factor (ARF)[15,16] transcriptional activators[16,17]. When auxin levels rise, the Aux/IAA proteins are degraded by the 26S proteasome[18], resulting in derepression of ARFs and activation of transcriptional responses[19]. In *Arabidopsis*, 29 Aux/IAA proteins have been identified, most of which share a similar domain structure. Domain I (DI) binds TOPLESS and is required for transcriptional repression. Domain II (DII) contains the degron motif, a sequence of 13 amino acids that is required for the characteristic instability of Aux/IAA proteins. Domains III and IV mediate homo- and heterodimerization, including interactions with ARF proteins[11]. As synthesis of many Aux/IAA proteins themselves is rapidly induced by auxin, auxin signaling undergoes cycles of negative feedback regulation[20,21].

Auxin-dependent degradation of the Aux/IAAs occurs through the action of a SKP1–Cullin–F-box (SCF)-type E3 ligase called SCF^{TIR1/AFB1–5}. The F-box protein TIR1 and the related proteins AFB1, AFB2, AFB3, AFB4 and AFB5 are the substrate-specificity determinants, or substrate receptors, for the SCF[22–24].

Unexpectedly, substrate recognition requires direct binding of auxin to the F-box protein[24–26]. Along with the identification of a long-sought mechanism of auxin perception, this was the first demonstration of an SCF-substrate interaction that is regulated by the direct binding of a small ligand. The structure of TIR1 was determined in the presence of auxin and a 13-amino-acid degron peptide from DII of Aux/IAA protein IAA7 (refs. 27,28). The resulting model reveals key aspects of TIR1-auxin binding as well as the TIR1-Aux/IAA interaction. First, the model shows that the mushroom-like fold of the TIR1–Arabidopsis SKP1-like (ASK1) complex, formed by the 18 leucine-rich repeats in the C terminus of TIR1, is essential for Aux/IAA and auxin binding. Second, it confirms that post-translational modifications are not required for auxin or Aux/IAA binding to TIR1. Third, it reveals that auxin binding to TIR1 does not result in changes in TIR1 conformation. Rather, auxin seems to function by extending the protein-interaction interface and increasing the affinity of TIR1 for the Aux/IAA protein. This view is supported by the fact that auxin occupies the binding pocket in TIR1, just underneath the Aux/IAA binding site. Last, it reveals that an inositol 1,2,3,4,5,6-hexakisphosphate ($InsP_6$) cofactor is bound at the core of TIR1.

Pull-down experiments indicate that all six members of the TIR1/AFB family function as auxin receptors. However, a number of studies have shown that individual TIR1/AFB proteins have distinct biochemical properties and biological functions. For example, TIR1 and AFB2 have a much stronger interaction with Aux/IAA proteins than AFB1 and AFB3 (refs. 24,29). AFB3 has been shown to have a unique role in the nitrate response of roots[30]. In addition, genetic experiments indicate that AFB4 negatively regulates the auxin response, unlike other members of the family[29].

[1]Section of Cell and Developmental Biology, University of California–San Diego, La Jolla, California, USA. [2]Howard Hughes Medical Institute (HHMI), University of California–San Diego, La Jolla, California, USA. [3]School of Life Sciences, University of Warwick, Coventry, UK. [4]Department of Chemistry and Biochemistry, University of California–San Diego, La Jolla, California, USA. [5]Bioorganic Chemistry Department, IPB–Leibniz Institute of Plant Biochemistry, Halle (Saale), Germany. [6]Centre for Plant Sciences, University of Leeds, Leeds, UK. [7]Department of Pharmacology, University of Washington, School of Medicine, Seattle, Washington, USA. [8]Howard Hughes Medical Institute, University of Washington School of Medicine, Seattle, Washington, USA. [9]Department of Plant Sciences, University of Liverpool, Liverpool, UK. [10]Present addresses: Molecular Signal Processing Department, IPB–Leibniz Institute of Plant Biochemistry, Halle (Saale), Germany (L.I.A.C.V.); Center for Genetics and Genomics, Harvard Medical School, Boston, Massachusetts, USA (X.T.). [11]Deceased. *e-mail: mestelle@ucsd.edu
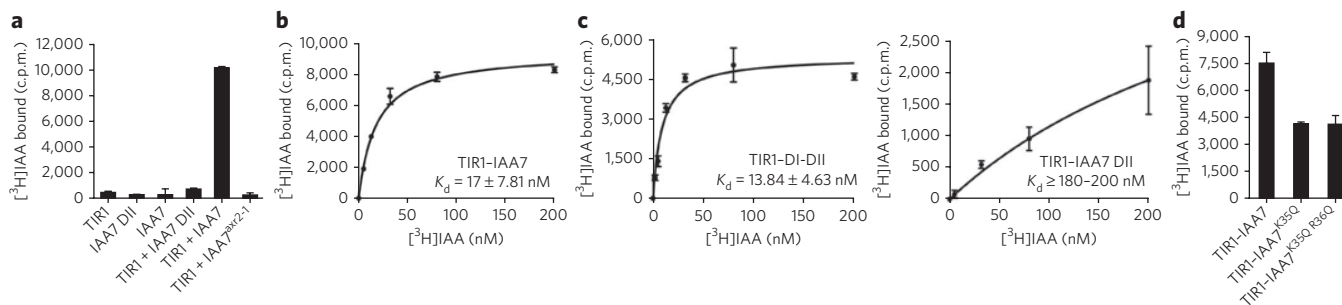
Figure 1 | The auxin receptor is a co-receptor system. (**a**) *In vitro* binding of 200 nM [³H]IAA to recombinantly expressed TIR1 and/or full-length IAA7 or a peptide corresponding to the IAA7 DII degron motif. Together, the TIR1–IAA7 pair constitutes an auxin co-receptor. A mutation that mimics a gain-of-function allele in the degron of IAA7 (IAA7[axr2-1]) abolishes auxin binding. (**b,c**) Saturation binding experiments of [³H]IAA to TIR1–IAA7 (**b**), which constitutes a high-affinity auxin co-receptor with a K_d in the low nanomolar range, and to TIR1–DI-DII (**c**, left) and TIR1–IAA7 DII co-receptor complexes (**c**, right). TIR1–DI-DII but not TIR1–IAA7 DII binds auxin with high affinity in **c**. (**d**) [³H]IAA binding at 200 nM to TIR1–IAA7 compared to TIR1–IAA7[K35Q] and TIR1–IAA7[K35Q R36Q]. Values are determined as mean ± s.e.m. of either two or three independent experiments carried out in triplicate.

Although advances have been made in our understanding of auxin perception, a number of key uncertainties remain, including the nature of the auxin receptor itself. For example, it is not clear whether TIR1/AFB receptors can bind auxin alone or whether the Aux/IAA protein also contributes to auxin binding. Similarly, the binding properties of individual TIR1/AFB proteins for different auxins and Aux/IAA proteins have not been systematically determined. In this study, we use a variety of biochemical approaches to resolve these issues. Our results demonstrate both the remarkable complexity and the diversity of the auxin perception mechanism.

RESULTS
TIR1 and Aux/IAA proteins act as auxin co-receptors
To evaluate the molecular requirements of auxin binding, we carried out *in vitro* auxin binding assays using [³H]IAA. For these experiments, we expressed a tagged version of TIR1 together with ASK1 in Hi5 insect cells[28]. TIR1–ASK1 was incubated with labeled IAA and either a synthetic peptide derived from domain II of IAA7 (IAA7 DII)[22] or full-length IAA7. We found that TIR1, the IAA7 DII and IAA7 all lacked appreciable binding to IAA, whereas the combination of TIR1 together with a molar excess of IAA7 DII peptide showed relatively low binding to auxin (**Fig. 1a**). In strong contrast, TIR1 with full-length IAA7 bound auxin with high affinity ($K_d = 17.81 \pm 7.81$ nM; **Fig. 1b**). We also evaluated auxin binding to TIR1 in combination with a mutated version of IAA7 that carries a P87S substitution in DII (IAA7[axr2-1]). This mutation corresponds to a dominant mutation that stabilizes IAA7 *in vivo* (called *axr2-1*) and abolishes the TIR1–Aux/IAA interaction[31,32]. The TIR1–IAA7[axr2-1] combination did not bind auxin, confirming that both proteins are required for substantial binding (**Fig. 1a**).

To further investigate the contribution of the Aux/IAA protein to auxin binding, we carried out binding experiments using TIR1 together with truncated versions of IAA7 containing the DI and DII domains (DI-DII) or DII only. Saturation binding assays showed that the TIR1–DI-DII complex binds auxin with an affinity similar to that of TIR1–IAA7 ($K_d = 13.84 \pm 4.63$ nM) (**Fig. 1c**). In contrast, the TIR1–IAA7 DII combination had a binding affinity one order of magnitude lower ($K_d = 218.40 \pm 25.80$ nM) than the TIR1–IAA7 combination. This result is in agreement with the results of surface plasmon resonance (SPR) experiments done with TIR1 and an immobilized DII peptide, in which we obtained a binding affinity for IAA of 111 nM (**Supplementary Results**, **Supplementary Fig. 2**). These results indicate that DII of the Aux/IAAs is essential for interaction with TIR1 but also indicate that other sequences within IAA7 contribute to complex formation. Previous studies show that a conserved lysine-arginine motif between DI and DII is

required for basal proteolysis of Aux/IAA proteins[20,33]. To determine the role of the lysine-arginine motif in auxin binding, we mutated Lys35 and Arg36 to glutamine and tested IAA binding. In both K35Q and K35Q R36Q mutants, auxin binding was diminished by ~50%, indicating that the lysine-arginine motif also contributes to assembly of the complex (**Fig. 1d**). Taken together, our *in vitro* auxin binding assays demonstrate that TIR1 and the Aux/IAA are both necessary and sufficient for auxin binding and act as auxin co-receptors (**Fig. 1a** and **Supplementary Fig. 1a**).

Co-receptor pairs assemble at different auxin concentrations
Previously, we showed that TIR1 and AFB1, AFB2 and AFB3 have similar but distinct roles in auxin signaling and speculated that these differences might relate to differential interactions with the Aux/IAA proteins[24]. To investigate this possibility, we analyzed a number of TIR1/AFB–Aux/IAA pairs in a yeast two-hybrid assay (Y2H) (**Fig. 2**). Nine Aux/IAA proteins representing distinct subclades[34] were chosen for this analysis. Seven of these contain the canonical Gly-Trp-Pro-Pro-Val (GWPPv; the small letter v indicates that valine is usually, but not always, conserved) degron motif, one (IAA31) contains a degenerate form of this motif and one (IAA20) completely lacks DII (**Fig. 2b**). The amount of heterologous proteins in yeast was assessed by immunoblot analysis showing that TIR1, AFB1, AFB2 and AFB5 fusion proteins were expressed at similar levels (**Supplementary Fig. 7**). The Aux/IAA proteins also accumulated to a roughly similar amount, allowing a qualitative assessment of their relative ability to form co-receptor complexes. Each co-receptor combination was evaluated on medium supplemented with increasing concentrations of auxin. Remarkably, we observed different dose-response relationships for different pairs of proteins. Among the Aux/IAAs tested, only IAA7 interacts with TIR1/AFBs in the absence of auxin. IAA5, IAA7 and IAA8 interact with all of the TIR1/AFBs at 0.1 μM IAA. IAA3 also bound TIR1, AFB1 and AFB2 at this concentration but was a poor substrate for AFB5. In contrast, IAA12, IAA28 and IAA29 required much higher concentrations of IAA to interact with the F-box proteins. IAA12 interacted specifically with TIR1 and AFB2 at 100 μM IAA, suggesting that, at least in the yeast system, higher concentrations of IAA are required to form stable TIR1– or AFB2–IAA12 complexes. The interaction between IAA28 and AFB2 or TIR1 was particularly strong at concentrations over 10 μM, whereas IAA29 interacted poorly and only at high IAA concentrations with AFB1 and AFB2 (**Fig. 2a**). Because all of these proteins include the GWPPv degron motif, our results suggest that additional amino acids, either within DII or elsewhere in the protein, contribute to the interaction with TIR1/AFBs (**Fig. 2b**). Additionally, the evolutionarily divergent IAA31 protein interacted weakly with
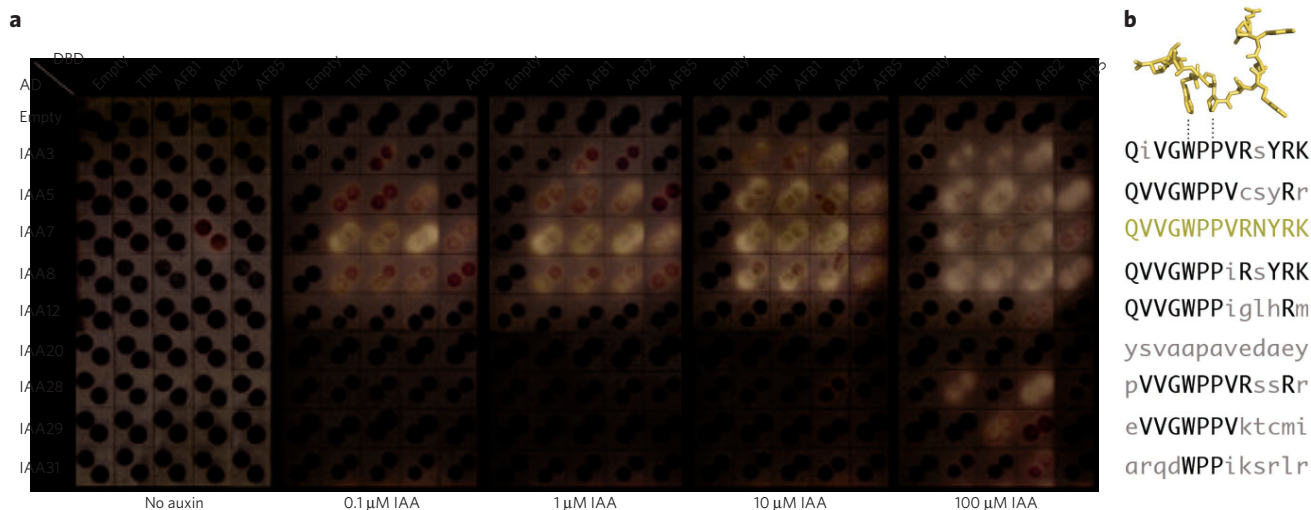
Figure 2 | Differences in auxin-dependent TIR1/AFB–Aux/IAA interaction are not exclusively determined by the degron domain. (**a**) Y2H interaction experiments of TIR1, AFB1, AFB2 and AFB5 with IAA3, IAA5, IAA7, IAA8, IAA12, IAA20, IAA28, IAA29 and IAA31, which represent the different subclades of *Arabidopsis* Aux/IAAs. Diploids containing LexA DBD–TIR1/AFBs and AD–Aux/IAAs were generated and spotted in selective medium containing increasing concentrations of IAA. β-galactosidase reporter expression evidenced IAA-induced protein-protein interactions 4 d after spotting. (**b**) Aux/IAA proteins with a very similar DII domain interact differentially with TIR1/AFBs, suggesting that regions outside of DII contribute to binding. IAA7 DII depicted as sticks (yellow) with conserved tryptophan and second proline residues, which interact with the surrounding hydrophobic wall in the TIR1 pocket and stack against the auxin molecule lying underneath. DII sequences of the selected Aux/IAAs in the Y2H from **a** and the canonical IAA7 DII (marked in yellow) are shown for comparison (right). Residues in capital letters represent a perfect match with the canonical degron..

the TIR1/AFBs. Finally, IAA20 did not interact with any of the TIR1/AFB proteins, even at high concentrations. This observation suggests that these Aux/IAAs are not substrates for SCF$^{TIR1/AFB}$ or that a different ligand is required to promote the interaction.

Overall, the results of our Y2H experiments suggest that there are substrate preferences among the TIR1/AFB proteins. Certain Aux/IAA proteins, such as IAA3, IAA5, IAA7 and IAA8, are generally better substrates for TIR1/AFBs than IAA12, IAA28 and IAA31.
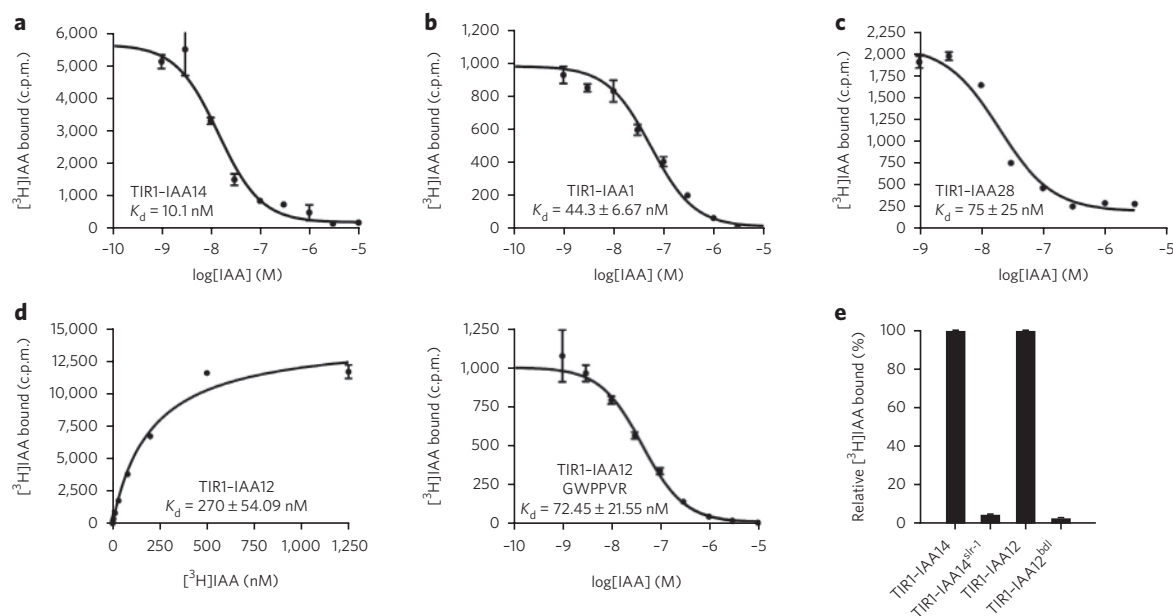

Figure 3 | Aux/IAA proteins determine the affinity of the co-receptor complex for auxin and, together with TIR1, form a series of co-receptor complexes with a range of auxin-sensing properties. (**a–c**) Homologous competitive binding experiments for TIR1–IAA14 (**a**), TIR1–IAA1 (**b**) and TIR1–IAA28 (**c**) co-receptor complexes. Specific binding of a constant concentration of [³H]IAA by the different co-receptors in the presence of various concentrations of unlabeled IAA was measured. IC_{50} values were determined using appropriate concentrations (5 nM, 10 nM, 25 nM or 100 nM) of radiolabeled auxin, so that the concentration of radiolabeled IAA was less than half the IC_{50}. K_d was then calculated as the IC_{50} of the [³H]IAA concentration fitted to a built-in equation of one-site competition. (**d**) Saturation binding of the TIR1–IAA12 co-receptor complex, which shows low auxin binding affinity in the high nanomolar range (left). The binding affinity of the TIR1–IAA12 co-receptor for IAA increases when the canonical degron motif GWPPVR is incorporated in IAA12 (right). (**e**) Mutated versions of Aux/IAA proteins that mimic the stabilized versions of the proteins (SOLITARY ROOT (*slr-1*) and BODENLOS (*bdl*)) abolish specific auxin binding by the different TIR1–Aux/IAA co-receptor complexes. Binding of [³H]IAA (200 nM) to recombinant TIR1–ASK1 and IAA14, IAA12, IAA14^{slr-1} and IAA12^{bdl}. Error bars correspond to s.e.m. of four replicates.

Table 1 | Auxin-binding activity of various auxin co-receptor complexes

Auxin co-receptor	DI and degron domain (DII) of Aux/IAA	Auxin	K_d or K_i* (mean ± s.e.m.) (nM)	n
TIR1–IAA7	KRGFSETVDLMLNLQSNKEGSVDLKNVSAVPKEKTTLKDPSKPPAKAQVVGWPPVRNYRKN MMTQQKTSS	IAA	17 ± 7.81	3
		1-NAA	113.50 ± 3.50	2
		2,4-D	248–1,000	4
		Picloram	3,900 ± 910	2
AFB5–IAA7	KRGFSETVDLMLNLQSNKEGSVDLKNVSAVPKEKTTLKDPSKPPAKAQVVGWPPVRNYRKN MMTQQKTSS	IAA	51.32 ± 12.65	3
		Picloram	54.70 ± 3.84	3
TIR1–IAA14	KRGFSETVDLKLNLQSNKQGHVDLNTNGAPKEKTFLKDPSKPPAKAQVVGWPPVRNYRKN VMANQKSGE	IAA	10.10	2
TIR1–IAA3	KRVLSTDTEKEIESSSRKTETSPPRKAQIVGWPPVRSYRKNNIQSKKNES	IAA	16.97 ± 3.43	3
TIR1–IAA17	KRGFSETVDLKLNLNNEPANKEGSTTHDVVTFDSKEKSACPKDPAKPPAKAQVVGWPPVR SYRKNVMVSCQKSS	IAA	33 ± 3.00	2
TIR1–IAA1	KRKNNDSTEESAPPPAKTQIVGWPPVRSNRKNNNN	IAA	44.33 ± 6.67	2
TIR1–IAA28	KRLELRLAPPCHQFTSNNNINGSKQKSSTKETSFLSNNRVEVAPVVGWPPVRSSRRNLTAQLKE	IAA	75 ± 25	2
TIR1–IAA12	KRSAESSSHQGASPPRSSQVVGWPPIGLHRMNSLVNNQA	IAA	270 ± 54.09	3
TIR1–IAA12 GWPPVR	KRSAESSSHQGASPPRSSQVVGWPPVRLHRMNSLVNNQA	IAA	72.45 ± 21.55	3
TIR1–IAA31	MEVSNSCSSFSSSSVDSTKPSPSESSVNLSLSLTFPSTSPQREARQDWPPIKSRLRDTLKGRRL	IAA	>1,000 (NF)	3
TIR1–DI-DII	MIGQLMNLKATELCLGLPGGAEAVESPAKSAVGSKRGFSETVDLMLNLQS NKEGSVDLKNVSAVPKEKTTLKDPSKPPAKAQVVGWPPVRNYRKNMMTQQKTSS	IAA	13.84 ± 4.63	2
TIR1-biotinylated peptide DII	AKAQVVGWPPVRNYRKN	IAA	218 ± 25.80	3

*K_d and K_i values were determined by nonlinear regression from saturation binding experiments and/or homologous competition binding assays, respectively. n, number of independent auxin binding assays performed in triplicates. NF, no fit. The underlined residues match the lysine-arginine motif and the canonical GWPPVR in DII of IAA7.

Our assays also indicate that the degron motif is necessary for co-receptor assembly but that other sequences probably contribute to complex formation.

Aux/IAA proteins determine co-receptor affinity for auxin

One of the more outstanding questions in auxin biology is how the hormone controls so many different aspects of plant growth and development. On the basis of the results of our Y2H analysis, it is possible that different TIR1/AFB–Aux/IAA co-receptor pairs have biochemical differences that enable specialized functions. For example, co-receptor pairs may have unique affinities for auxin and therefore respond to different auxin concentrations. To address this question, we carried out either saturation or homologous competitive IAA binding assays in which different TIR1–Aux/IAA combinations were incubated with a fixed concentration of radiolabeled IAA and increasing amounts of cold IAA (**Figs. 1** and **3** and **Supplementary Fig. 1b,c**). These experiments show that the binding affinity of IAA for the co-receptor complexes ranges from 10 nM to >1 µM. IAA14 is the closest IAA7 paralog, and the two proteins have an identical GWPPVR amino acid sequence in DII. Indeed, the TIR1–IAA14 co-receptor pair binds auxin with very high affinity (K_d ~10 nM), similarly to the TIR1–IAA7 co-receptor pair (**Fig. 3a** and **Table 1**). Interestingly, TIR1–IAA17 has a slightly lower affinity for IAA (K_d ~30 nM), even though IAA17 is closely related to IAA7 and has a nearly identical DII (**Table 1** and **Supplementary Fig. 1b**). The TIR1–IAA1 and TIR1–IAA3 co-receptor pairs have affinities between 17 nM and 45 nM for IAA, whereas TIR1–IAA28 binds auxin with a K_d of approximately 75 nM (**Fig. 3b,c**, **Table 1** and **Supplementary Fig. 1b**). Moreover, when we used stabilized DII mutant forms of the various Aux/IAA proteins in our binding assays, we observed that auxin binding was abolished independently of the binding properties of the native TIR1–Aux/IAA pair (**Fig. 3e**).

We next explored the auxin-binding capabilities of the TIR1–IAA12 pair as this complex assembles only at high auxin concentrations in Y2H assays (**Fig. 2a**). In accordance with the yeast results, the K_d for auxin of the TIR1–IAA12 co-receptor was 270.25 ± 54.09 nM, suggesting that this co-receptor has a comparatively low affinity for auxin (**Fig. 3d**).

To specifically determine the contribution of the canonical degron motif to the auxin binding affinity of the co-receptors, we mimicked the degron domain of IAA7 in IAA12 (IAA12 GWPPVR) and tested it in the auxin binding assay. Although TIR1–IAA12 GWPPVR showed an increased affinity for IAA (K_d = 72.45 ± 21.55 nM), we were not able to obtain K_d values equal to those observed for the TIR1–IAA7 co-receptor pair (**Figs. 1b** and **3d**). This is clear additional evidence that regions outside DII of Aux/IAA proteins also contribute to interaction with TIR1 and to auxin binding. Constitutively expressed fusions of DIIs of IAA8, IAA9 and IAA28 to VENUS fluorescent protein have been recently used as auxin sensors *in vivo*[35], but our results indicate that DI-DII of Aux/IAAs are required for the co-receptor to have full auxin-sensing properties. More importantly, our data show that Aux/IAA proteins determine the auxin binding properties of the TIR1–Aux/IAA co-receptor complex, which might allow the formation of a spectrum of auxin sensors.

TIR1 mutations affect co-receptor complex assembly

Structural studies have identified a number of key residues that participate in co-receptor assembly and auxin binding[28] (**Fig. 4a**). To explore the function of these residues, we generated mutant TIR1 proteins and evaluated their interaction with either ASK1 or IAA7 in Y2H assays (**Fig. 4b**). TIR1 and the AFBs interacted with ASK1 independently of auxin, and a mutant form of TIR1 that lacks the F-box motif was unable to interact with ASK1 (**Supplementary Fig. 3a**).
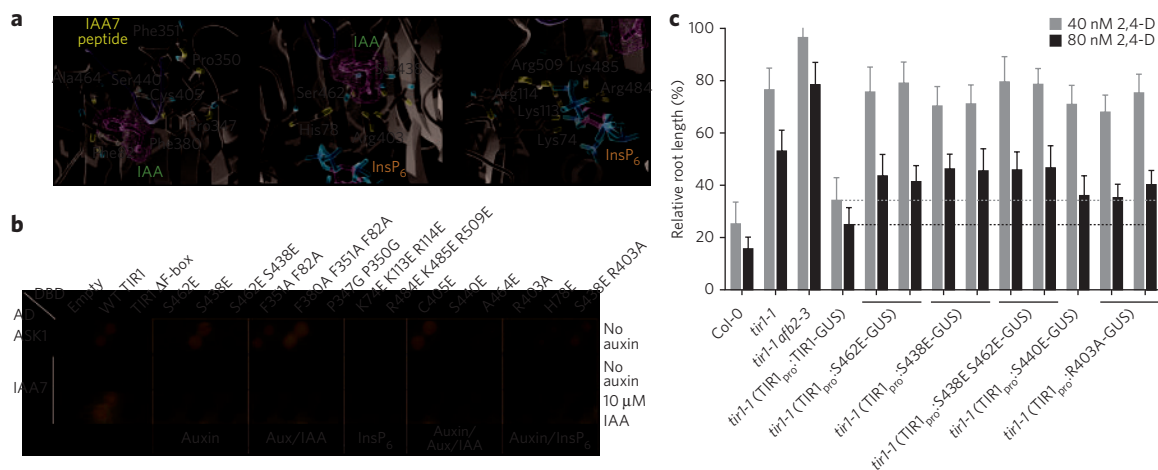
Figure 4 | Mutations at auxin, Aux/IAA and InsP$_6$ binding sites impair auxin-dependent TIR1–Aux/IAA interaction and compromise TIR1 function *in vivo*. (**a**) Side view of auxin (green) and IAA7 peptide (yellow) (left), auxin and InsP$_6$ (rainbow) (middle), and InsP$_6$ (right) binding sites in TIR1 (gray). Selected ligand-interacting residues in TIR1 are shown in mostly white stick representation. (**b**) Y2H ASK1 and auxin-induced IAA7 interactions with wild-type (WT) TIR1 or TIR1 carrying mutations on ligand-binding sites. (**c**) Five-day-old seedlings were transferred to growth medium containing either 40 nM or 80 nM 2,4-D. Root elongation was measured after an additional 4 d and expressed as a proportion of growth in the absence of auxin (error bars represent s.d.). Auxin inhibits root elongation in wild-type plants (Col-0), but *tir1-1* and the *tir1-1 afb2-3* auxin-receptor mutants are resistant to auxin treatment. Auxin resistance in *tir1-1* mutants is reverted by introducing wild-type TIR1 fused to the β-glucuronidase (*GUS*) reporter gene under the TIR1 promoter (TIR1$_{pro}$). Interrupted lines indicate that unlike TIR1$_{pro}$:TIR1-GUS, versions of TIR1 that carry mutations in ligand binding sites are unable to restore auxin sensitivity in *tir1-1* mutants.

Except for Ser440, residues implicated in auxin and/or Aux/IAA binding did not affect interaction with ASK1 when they were substituted. However, our studies showed that all of these residues are required for the auxin-dependent interaction of TIR1 with IAA7. Thus, substitution of residues within the auxin-binding groove (Ser462 and Ser438), residues that contribute to Aux/IAA interaction (Phe82, Phe351, Phe380, Pro347 and Pro350), residues that form the canopy of the auxin-binding groove (Cys405, Ser440 and Ala464) and residues that are implicated in both auxin and InsP$_6$ binding (His78, Arg403 and Ser438) all abolish interaction with IAA7 (**Fig. 4b**).

We also addressed the role of InsP$_6$ on TIR1 function (**Fig. 4a,b**). The InsP$_6$ binding pocket is surrounded by positively charged residues, including Lys74, Lys113, Arg114, Arg484, Lys485 and Arg509. These residues are thought to support the floor of the auxin-binding pocket. In addition, InsP$_6$ contacts Arg403, which interacts with the carboxyl group of auxin[28]. Two mutant proteins were generated, each of which replaced three of these residues with

glutamate. Both mutant proteins failed to interact with IAA7 in the presence of auxin in yeast and in pull-down experiments using tagged recombinant Aux/IAA protein (**Fig. 4b** and **Supplementary Fig. 3d**). This result is consistent with an important role for InsP$_6$ in TIR1 function. Further, neither mutant version of TIR1 was able to interact with ASK1 in yeast, suggesting that InsP$_6$ has a broader role in determining TIR1 architecture. Finally, we characterized mutant proteins previously identified in forward genetic screens using the Y2H assay[36,37]. The *tir1-1* and *tir1-2* mutations completely abolished the interaction between the mutant protein and either ASK1 or IAA7, suggesting that these substitutions result in major changes in protein structure (**Supplementary Fig. 3b**). In contrast, the *tir1-6*, *tir1-7* and *weak ethylene-insensitive* (*wei1*, also known as *tir1-101*) mutations have a modest effect on IAA7 interaction (**Supplementary Fig. 3c**), which correlates with the weaker phenotypes of these mutants.

To determine whether these mutant proteins function in plants, we introduced mutant versions of *TIR1* fused to the gene encoding
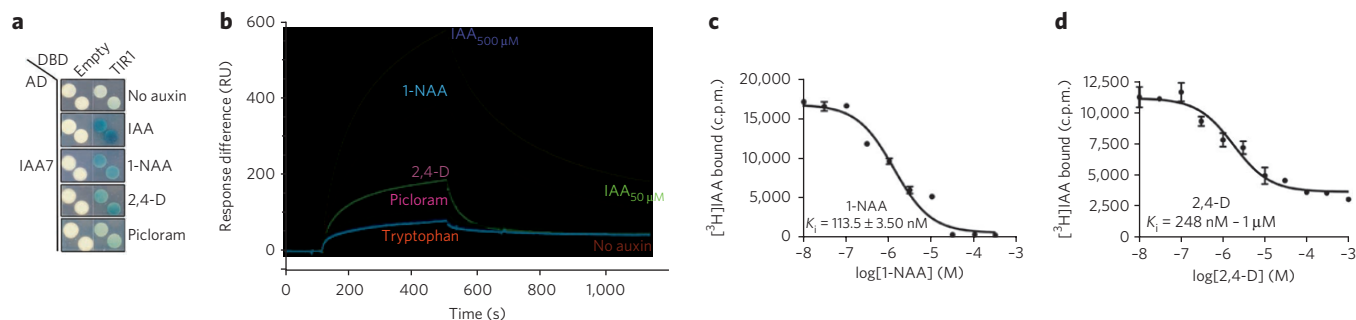

Figure 5 | Auxin agonists differentially stabilize TIR1–Aux/IAA complexes. (**a**) IAA, 1-NAA and 2,4-D enhance TIR1–IAA7 interaction in yeast. Diploids carrying LexA DBD-TIR1 and AD-IAA7 were spotted on selective medium containing 50 μM auxins. β-galactosidase expression is a measure of TIR1–IAA7 interaction. (**b**) SPR analysis of auxin-dependent TIR1–IAA7 DII interaction. Sensorgram shows the effect of no auxin and various auxinic compounds (500 μM IAA, 50 μM IAA, 50 μM 1-NAA, 50 μM 2,4-D, 50 μM picloram, 50 μM tryptophan) on TIR1-DII peptide association and dissociation. Auxins were mixed with TIR1 in solution before injection over DII peptide. RU, resonance units. (**c,d**) Competitive [^{3}H]IAA binding assays using 1-NAA (**c**) and 2,4-D (**d**) cold competitors. TIR1–IAA7 co-receptor complex binds 1-NAA and 2,4-D with a K_i (inhibition constant) of 113.50 ± 3.51 nM and >1 μM, respectively.
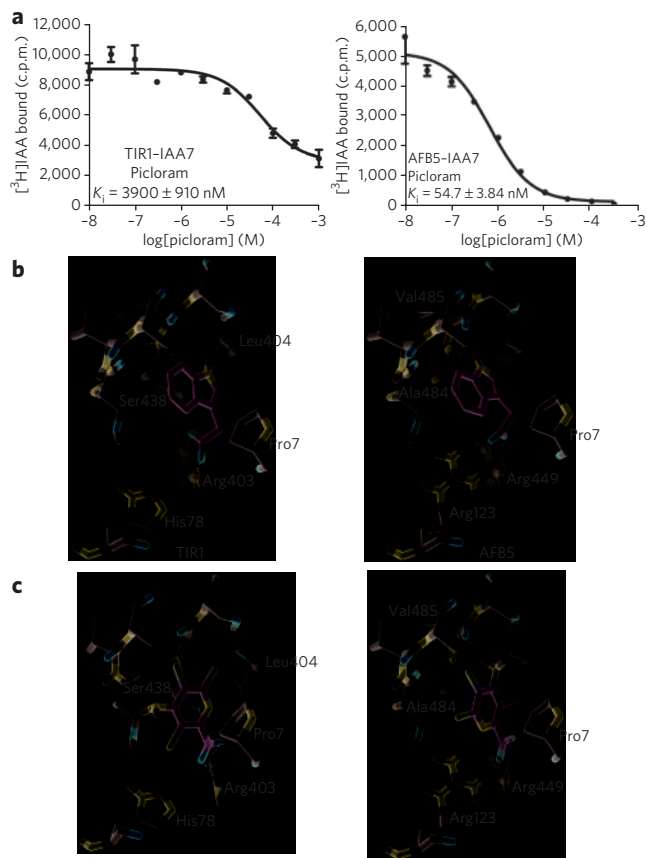
Figure 6 | TIR1–IAA7 and AFB5–IAA7 co-receptor complexes have differential auxin-binding affinities. (**a**) Heterologous competition binding experiments of TIR1–IAA7 and AFB5–IAA7 co-receptor complexes. Picloram efficiently displaces [³H]IAA binding by AFB5–IAA7, but not by the TIR1–IAA7 complex. (**b,c**) Three-dimensional structures of TIR1 and AFB5 show an almost identical fold with regard to secondary structure arrangements. Docking arrangements of IAA to TIR1 (left) and AFB5 (right) (**b**) and of picloram to TIR1 (left) and AFB5 (right) (**c**). IAA and picloram are stabilized in the TIR1 auxin-binding pocket by hydrogen bonds to Arg403 (left side of **b** and **c**). IAA and picloram form strong hydrogen bonds (salt bridges) to Arg123 and Arg449 and to the backbone carbonyl group of Val485 in AFB5 (right side of **b** and **c**). In **b**, picloram lacks the hydrogen bond to the backbone carbonyl group of Leu404 in TIR1. The replacement of Arg123 (in AFB5) by His78 (in TIR1) is most likely responsible for the reduced affinity of picloram to TIR1 compared to AFB5, as shown in **c**.

β-glucuronidase (GUS) under control of the *TIR1* promoter into wild-type and *tir1-1* plants (**Fig. 4c**). We previously showed that expression of a *TIR1* cDNA from the *TIR1* promoter rescues the auxin-resistant phenotype of *tir1-1* plants in root-elongation assays[24]. We introduced single and double mutations affecting putative auxin and Aux/IAA binding sites, including S438E, S462E, S440E or R403A. At least four transgenic lines were identified for each mutation and were characterized with respect to GUS expression and auxin response. None of the transgenes were able to restore auxin sensitivity to *tir1-1* plants. This observation suggests that the TIR1 mutant proteins are not functional and indicates that Ser438, Ser462, Ser440 and Arg403 are essential for TIR1 function *in planta* (**Fig. 4c**). In summary, mutagenesis of TIR1 provides strong support for the published structural model[28]. Our data indicate that TIR1–Aux/IAA co-receptor formation and interaction with ASK1 are essential for auxin sensing *in vivo*.

Auxin agonists differentially stabilize TIR1–Aux/IAA

The auxin-binding groove of TIR1 consists of a three-walled hydrophobic cavity with an open roof and two selective polar residues that anchor the auxins to the base of the pocket[28]. The pocket can accommodate various auxin analogs including 1-NAA and 2,4-D. Moreover, other studies have shown that various chemically diverse compounds have auxin agonist as well as antagonist activity[9,38,39]. The synthetic auxins 1-NAA, 2,4-D and picloram show auxin activity in a wide range of physiological responses and promote TIR1/AFB–Aux/IAA interactions *in vitro*[39]. We asked whether the synthetic auxins 1-NAA, 2,4-D and picloram promote TIR1–Aux/IAA interaction in yeast. We observed that all three auxins promoted TIR1–IAA7 interaction, but not to the same extent as IAA (**Fig. 5a**). We next tested the contribution of the different auxins to the TIR1–Aux/IAA dynamic interaction using SPR analyses. In this experiment, we evaluated the kinetics of co-receptor complex formation using an immobilized biotinylated peptide corresponding to the degron motif of IAA7 (DII) and purified TIR1 protein, in the absence or presence of different auxins. A small amount of basal binding occurred between TIR1 and the IAA7 DII peptide in the absence of auxin. In contrast, injection of TIR1 together with IAA, NAA, 2,4-D and picloram enhanced association with the peptide. Intriguingly, we also observed that the dissociation rate of the complexes differed, depending on the auxin in the system (**Fig. 5b**). When comparing the sensorgrams at 50 μM ligand concentration, little difference is observed between the effects of IAA and NAA on TIR1–DII association, whereas 2,4-D addition led to a much more rapid dissociation rate. This accounts for the apparent reduction in maximum binding capacity (R_{max}) by working against association of the complex. TIR1–IAA7 DII complex formation with picloram was weaker and showed rapid dissociation. We carried out heterologous competitive binding experiments for comparison and determined that the TIR1–IAA7 co-receptor complex has a higher binding affinity for 1-NAA than for 2,4-D (K_d = 113.50 ± 3.50 nM and K_d between 248 nM and 1 μM, respectively; **Fig. 5c,d** and **Table 1**). Taken together, our data show that distinct auxins differentially stabilize the TIR1–IAA7 co-receptor complex and that an important determinant of affinity is the dissociation rate. Our previous TIR1 structural studies show that IAA, 1-NAA and 2,4-D are anchored in the binding pocket through interactions between their carboxylate group and the TIR1 residues Arg403 and Ser438 (ref. 28). However, only IAA establishes an additional connection to the walls of the pocket through an interaction between the NH group of the indole ring of IAA and Lys439 of TIR1. Owing to its double aromatic rings, 1-NAA provides a larger hydrophobic platform for association with the auxin-binding pocket of TIR1 than 2,4-D[28]. Computational comparative analysis of hydrogen-bond energy formation of TIR1–IAA7 and various auxins has also suggested that IAA forms stronger bond interactions with the co-receptor[40]. This is consistent with the slower dissociation rate observed for the TIR1–IAA–IAA7 DII complex.

The AFB5–IAA7 co-receptor complex binds picloram

AFB4 and AFB5 have diverged substantially from the other members of the TIR1/AFB family[24]. Previous studies indicate that *afb5* mutant plants are resistant to the synthetic auxin picloram, whereas *tir1* plants are not, suggesting that AFB5 shows agonist selectivity[41]. Recently, we presented evidence that both *afb4* and *afb5* are resistant to picloram and that the AFB4 clade may be the major target for this class of herbicides[29]. To investigate the biochemical basis for this selectivity, we compared the auxin binding affinity of AFB5–IAA7 to that of TIR1–IAA7. In competition binding assays, we evaluated the binding of radiolabeled IAA to either TIR1–IAA7 or AFB5–IAA7 in the presence of increasing concentrations of unlabeled picloram (**Fig. 6a**). We found that though the AFB5–IAA7 co-receptor complex has a relatively high affinity for picloram (K_i = 54.90 ± 3.84 nM),

picloram was not able to displace IAA efficiently from TIR1–IAA7 (K_i = 3,900 ± 910 nM). These results provide evidence for AFB5 selectivity and an explanation for the picloram resistance of *afb4* and *afb5* mutant plants. Further, we evaluated the ability of the AFB5–IAA7 co-receptor to bind IAA. Saturation binding curves show that AFB5–IAA7 binds IAA with a K_d of 51.32 ± 12.65 nM, similar to the AFB5–IAA7 affinity for picloram and resembling to some degree binding of TIR1–IAA7 to IAA (K_d ~10 nM) (**Table 1** and **Supplementary Fig. 4b**). Next, we compared the kinetics of association and dissociation of the AFB5–IAA7 and TIR1–IAA7 complexes in SPR experiments in the presence of various auxins, including picloram. We found that picloram promotes rapid assembly of the AFB5–IAA7 complex and, to a lesser extent, the TIR1–IAA7 complex, although dissociation dominates the extent of complex assembly for AFB5–IAA7. Indeed, we found that dissociation of the AFB5–IAA7 complex was more rapid than that of TIR1–IAA7, irrespective of the auxin (**Supplementary Fig. 4c**).

To address differences in the TIR1–IAA7 and AFB5–IAA7 co-receptor complexes, we built a structural model of the AFB5 protein by homology modeling using the *Arabidopsis* TIR1 structure as a template (**Fig. 6b,c** and **Supplementary Fig. 5**). AFB5 differs from TIR1 at two positions in the auxin-binding pocket: His78 and Ser438 in TIR1 are replaced by Arg123 and Ala484, respectively, in AFB5. We carried out docking calculations of IAA in AFB5 and picloram in TIR1- and AFB5-binding pockets (**Fig. 6b,c**). The simulations indicated that the histidine-arginine exchange has a strong influence on the docking arrangements and affinities of TIR1 and AFB5 for IAA and picloram. Despite differences in their ring structure and although their electrostatic interactions differ, picloram, IAA and 2,4-D oriented in the cavity in a similar way (**Fig. 6b,c**). However, their electrostatic interactions differed. In TIR1, Arg403 tethers the carboxylate of picloram (and other auxins) through a salt bridge to the bottom of the auxin-binding pocket. By contrast, AFB5 Arg123 and Arg449 (TIR1 Arg403 equivalent) establish strong salt bridges with the carboxylate group of auxin. In addition, in AFB5, the imino group of IAA and the amino group of picloram form a hydrogen bond to the backbone carbonyl group of Val485. Hydrophobic interactions of the aromatic ring systems with Pro7 of IAA7 DII further stabilize the docking arrangements for auxins in AFB5 (**Fig. 6b,c**). These simulations largely support our binding experiments and show that the affinity of AFB5 for picloram is nearly as high as that of TIR1 for IAA (**Fig. 6b,c** and **Supplementary Fig. 4**). Taken together, these data clearly show that AFB5 acts as a high-affinity sensor for IAA and has a stronger binding affinity for picloram. Further detailed studies will directly establish the basis for this selectivity further.

DISCUSSION

Recent studies have produced a new view of auxin perception. Biochemical and structural experiments indicate that auxin acts directly to promote an interaction between the F-box protein TIR1 and the Aux/IAA transcriptional repressors. However, many details of the mechanism of auxin perception remain to be elucidated. Here we used a variety of approaches to perform a detailed characterization of the auxin receptor.

The structural model of TIR1 implicated a number of residues in auxin, Aux/IAA and InsP$_6$ binding. When we investigated the function of these residues in genetic studies, we found that these amino acids are essential for TIR1 structure and/or function in both yeast and *Arabidopsis*.

On the basis of our initial studies, we proposed that auxin may act by binding to both TIR1 and the Aux/IAA protein, thus stabilizing the SCF^{TIR1}–Aux/IAA complex[25,28]. To test this possibility, we performed auxin binding assays with purified proteins. Our results show that high-affinity auxin binding requires the assembly of an auxin co-receptor complex consisting of TIR1 and an Aux/IAA protein. Further, we found that auxin binding to the combination of TIR1 and the IAA7 DII was one order of magnitude weaker than binding to TIR1 and full-length Aux/IAA protein, indicating that sequences outside DII contribute to complex formation.

The auxin co-receptor model has important implications. As there are 29 Aux/IAA proteins in *Arabidopsis*, it is possible that a number of qualitatively different co-receptor pairs may exist. Our Y2H results strongly suggest that this is the case. We observed variation in the auxin dose response for a number of the TIR1/AFB–Aux/IAA receptor pairs. Remarkably, the strength of the TIR1–Aux/IAA interaction inversely correlates with Aux/IAA stability. For example, IAA7 has a very strong interaction with TIR1/AFBs in yeast and has a half-life of ~10 min in *Arabidopsis* upon auxin treatment[23]. In contrast, IAA31, a relatively stable Aux/IAA, interacts poorly with the TIR1/AFBs. Although the yeast experiments provide information on the relative affinity of different co-receptor pairs for auxin, the results are not quantitative. As IAA is transported out of yeast cells and is probably metabolized as well, the intracellular IAA concentration is uncertain[42]. In addition, it has been shown that Aux/IAA proteins are degraded in yeast cells expressing TIR1 in the presence of auxin[43].

Our *in vitro* studies provide direct evidence that different co-receptor pairs have different auxin-binding affinities. The K_d for IAA among the co-receptor pairs ranges from ~10 nM in the case of TIR1–IAA7 to ~300 nM for TIR1–IAA12 and >1 μM for TIR1–IAA31 using full-length Aux/IAAs. To determine whether changes in IAA7 DII alone are responsible for differences in affinity, we mutated this domain in IAA12 to match the sequence of IAA7. This change substantially increased the IAA affinity of the TIR1–IAA12 pair, but not to the level of TIR1–IAA7. Further, we found that mutation of the conserved lysine-arginine motif, located between DI and DII, notably reduces IAA affinity.

The variation in binding affinity among the co-receptor pairs noticeably increases the dynamic range of auxin sensitivity. Thus, we would expect TIR1–IAA7 to respond to very low IAA concentration, whereas IAA12 would be degraded only at IAA concentrations in the high nanomolar range. Accordingly, *axr2* mutants expressing a stable version of IAA7 show an altered growth response to an extremely low concentration of auxin[44], suggesting that IAA7 mediates responses to low hormone concentrations. On the other hand, IAA12/BODENLOS protein has an important function during embryogenesis when localized surges of auxin regulate development of the apical-basal axis and formation of the root and shoot meristems[3,45]. We would expect TIR1–IAA12 to be responsive to the high IAA concentrations that result from these surges. In this regard, however, it is also important to note that we have not excluded the possibility that IAA12 has a high affinity for one of the other AFB proteins.

According to our yeast data, the IAA affinity of the co-receptor seems determined primarily by the Aux/IAA protein and not by the F-box protein. There are a few exceptions to this rule. For example, IAA28 paired with AFB2 has a higher apparent affinity than TIR1, AFB1 or AFB5, whereas IAA29 produces the strongest response with AFB1. More remarkable is the behavior of AFB5. Our results support earlier genetic studies indicating that AFB5 has a specific interaction with the synthetic auxin picloram. Our experiments revealed that the AFB5–IAA7 complex has a much higher affinity for picloram than TIR1–IAA7. Homology modeling suggests that this difference may be related to substitution of His78 in TIR1 with Arg123 in AFB5.

In summary, we have shown that auxin is sensed by a co-receptor complex consisting of a TIR1/AFB protein and an Aux/IAA protein. We also determined that both protein partners contribute to ligand selectivity. Additionally, we showed that different co-receptor complexes show very different affinities for auxin, dramatically increasing the dynamic range of the hormone. This most likely contributes to the versatility of auxin as a signaling molecule throughout plant growth and development.

METHODS

Plant materials and growth assays. Wild-type Columbia (Col-0) and *tir1-1* transgenic *Arabidopsis* plants expressing the TIR1 promoter (TIR1$_{pro}$):TIR1-GUS were described previously[24]. Various mutated versions of TIR1 were introduced by site-directed mutagenesis into the TIR1 cDNA cassette in the TIR1$_{pro}$:TIR1-GUS construct, and wild-type as well as *tir1-1* plants were transformed and selected on hygromycin. At least four T2-generation lines were used for root elongation assays (**Supplementary Methods**).

LexA Y2H assays. Y2H assays were carried out as in ref. 34. DNA-binding domain (DBD)-AFB1–5 and activation domain (AD) Aux/IAA constructs were generated and tested as described in **Supplementary Methods**.

[³H]-labeled auxin binding assay. Radioligand binding assays were performed using purified ASK1–TIR1 and ASK1–AFB5 protein complexes recombinantly expressed in insect cells as in ref. 28. Glutathione *S*-transferase (GST) tagged Aux/IAAs or their dominant mutated versions were expressed in *Escherichia coli*. In brief, in a typical auxin binding assay, 0.44 µg of ASK1–TIR1 or ASK1–AFB5 complex and a 1:10 molar radio of Aux/IAA proteins were incubated in 100 µl binding buffer (50 mM Tris-HCl (pH 8.0), 200 mM NaCl, 10% (v/v) glycerol, 0.1% (v/v) Tween 20, protease inhibitors) with 200 nM [³H]IAA for >1 h at 4 °C. [³H]IAA with a specific activity of 20 Ci mmol^{-1} from American Radiolabeled Chemicals was used. The samples were immobilized in polyethyleneimine pretreated fiberglass filters and washed three times with binding buffer. Upon overnight incubation, auxin binding was quantified by scintillation counting. Nonspecific binding was determined using a 1,000-fold excess of cold IAA with respect to [³H]IAA. Specific binding was determined as the average of at least three measurements of total binding minus nonspecific binding. For saturation binding assays, samples were prepared as above and incubated with at least six IAA concentrations on either side of the K_d of a given co-receptor pair. For homologous and nonhomologous competition binding assays, various concentrations of cold IAA, 1-NAA, 2,4-D and picloram were added to the samples containing a fixed concentration of [³H]IAA. Depending on the estimated IC$_{50}$ of the competitive compound, 5 nM, 10 nM, 25 nM or 100 nM of [³H]IAA was used. For competitive binding assays, K_d and K_i values were obtained by fitting the normalized specific binding affinity versus the logarithm of the unlabeled auxin concentration (log[IAA], M) using the one-site competition model. Nonlinear regression in Prism 5 (GraphPad Software) was used for all data analysis.

SPR. SPR measurements were performed using Biacore 2000 and Biacore 3000 systems (Biacore GE Healthcare Biosciences). Biotinylated IAA7 DII peptide (biotin-AKAQVVGWPPVRNYRKN) or respective Aux/IAA DII peptides were immobilized onto a streptavidin-coated Biacore SA sensor chip in sample cell. Reference cell was either blocked with a mutated version of IAA7 DII (biotin-AKAQVV**EWSSG**RNYRKN, where underlining indicates residues differing from the wild-type peptide) as negative control or coated with biocytin. Purified ASK1–TIR1 or ASK1–AFB5 proteins were injected over the chip at a flow rate of 25 µl min^{-1} in HBS-EP buffer (20 mM HEPES (pH 7.4), 150 mM NaCl, 3.4 mM EDTA and 0.005% (w/v) P20 surfactant) ± various concentrations of either IAA, 1-NAA, 2,4-D, picloram or tryptophan. Data analysis was performed with BIAevaluation software (GE Healthcare–Biacore Life Sciences).

Aux/IAA peptides. For radioligand binding assays, biotinylated peptides corresponding to the wild-type and mutated degron domain of IAA7 were purchased from Midwest Bio-Tech. Five milligrams of biotin (long-chain) AKAQVVGWPPVRNYRKN and biotin (long-chain) AKAQVVGWSPVRNYRN peptides were synthesized to a purity of 90–95% by HPLC according to manufacturer instructions. For SPR analyses, biotinyl-(NH)-AKAQVVGWPP VRNYRKN-(COOH) and mutant peptide biotinyl-(NH)-AKAQVV**EWSSG** RNYRKN-(COOH) were synthesized by Thermo Fisher Scientific to >80% purity (generally 94–95% pure).

Homology modeling of AFB5. AFB5 was modeled using the Prime module of the Schrodinger 2010 software package[46], using the *Arabidopsis* TIR1 structure as a template (Protein Data Bank (PDB) code 2P1Q: chain B). After pairwise sequence alignment (**Supplementary Fig. 6a**), a model structure was built, followed by side chain optimization and energy minimization. The quality of the model was first analyzed with PROCHECK[47]. The Ramachandran plot showed 88.3% of all backbone dihedral angles in most favored areas, 10.5% in additional allowed ones, three amino acids in generally allowed areas and one outlier (Ser298) appeared (**Supplementary Fig. 5a**). As the corresponding values are slightly better for the template X-ray structure of TIR1 (PDB code 2P1Q: chain B) (90.5% and 9.3%, respectively, with no outlier), the model was refined with the molecular dynamics refinement tool of YASARA using the YASARA2 force field. The resulting structure was slightly improved with regard to the Ramachandran plot analysis. An outlier was no longer detected, 89.1% of all backbone dihedral angles were in the most favored area and 10.5% were in additionally allowed ones. All other criteria, such as planarity of peptide bonds, bond length and angles for high stereochemical quality obtained by the PROCHECK analysis, were fulfilled. To analyze the model

structure for a putative native fold, an analysis with PROSA II was performed[48] (**Supplementary Fig. 5b**). The energy graph is almost identical to the X-ray structure template. The resulting combined Z-score value for the model of AFB5 with 566 amino acids is −13.85, which is close to −14.30, the score of the X-ray structure with 571 amino acids. This result is a strong indication for a native-like folded model structure. Both three-dimensional structures show an almost identical fold with regard to secondary structure arrangements.

Molecular modeling of interactions between picloram and TIR1 and AFB5. Automated docking simulations were performed with the algorithm-based induced-fit docking protocol of the Schrödinger suite. Prior to the calculation, each of the protein and ligand structures was prepared by adding hydrogens according to the expected protonation at pH 7, using the protein preparation and ligand preparation wizards available within Maestro. The best docking poses were selected by conformational clustering analysis and by binding score. The refined AFB5 structure and the TIR1 structure (after being three-dimensionally protonated with Molecular Operating Environment[49]) were taken for docking of IAA and picloram as ligands using the Protein-Ligand ANT System (PLANTS) with the ChemPLP scoring function and the Lennard Jones potential for intra-ligand energy calculations[50]. For each ligand and protein, 30 docking poses were calculated from which the most favored (lowest docking scores) were compared (**Supplementary Fig. 6b**).

References

1. Weijers, D., Ljung, K., Leyser, O. & Estelle, M. *Auxin Signaling: From Synthesis to Systems Biology* (ed. Estelle, M.) (Cold Spring Harbor Laboratory Press, 2011).
2. Hamann, T., Benková, E., Baurle, I., Kientz, M. & Jurgens, G. The *Arabidopsis* BODENLOS gene encodes an auxin response protein inhibiting MONOPTEROS-mediated embryo patterning. *Genes Dev.* **16**, 1610–1615 (2002).
3. Weijers, D. *et al.* Auxin triggers transient local signaling for cell specification in *Arabidopsis* embryogenesis. *Dev. Cell* **10**, 265–270 (2006).
4. Holland, J.J., Roberts, D. & Liscum, E. Understanding phototropism: from Darwin to today. *J. Exp. Bot.* **60**, 1969–1978 (2009).
5. Scarpella, E., Barkoulas, M. & Tsiantis, M. Control of leaf and vein development by auxin. *Cold Spring Harb. Perspect. Biol.* **2**, a001511 (2010).
6. Vernoux, T., Besnard, F. & Traas, J. Auxin at the shoot apical meristem. *Cold Spring Harb. Perspect. Biol.* **2**, a001487 (2010).
7. Overvoorde, P., Fukaki, H. & Beeckman, T. Auxin control of root development. *Cold Spring Harb. Perspect. Biol.* **2**, a001537 (2010).
8. Sundberg, E. & Østergaard, L. Distinct and dynamic auxin activities during reproductive development. *Cold Spring Harb. Perspect. Biol.* **1**, a001628 (2009).
9. Woodward, A.W. & Bartel, B. Auxin: regulation, action, and interaction. *Ann. Bot.* **95**, 707–735 (2005).
10. Abel, S. & Theologis, A. Early genes and auxin action. *Plant Physiol.* **111**, 9–17 (1996).
11. Overvoorde, P.J. *et al.* Functional genomic analysis of the AUXIN/INDOLE-3-ACETIC ACID gene family members in *Arabidopsis thaliana*. *Plant Cell* **17**, 3282–3300 (2005).
12. Tiwari, S.B., Wang, X.J., Hagen, G. & Guilfoyle, T.J. AUX/IAA proteins are active repressors and their stability and activity are modulated by auxin. *Plant Cell* **13**, 2809–2822 (2001).
13. Long, J.A., Ohno, C., Smith, Z.R. & Meyerowitz, E.M. TOPLESS regulates apical embryonic fate in *Arabidopsis*. *Science* **312**, 1520–1523 (2006).
14. Szemenyei, H., Hannon, M. & Long, J.A. TOPLESS mediates auxin-dependent transcriptional repression during *Arabidopsis* embryogenesis. *Science* **319**, 1384–1386 (2008).
15. Okushima, Y. *et al.* Functional genomic analysis of the AUXIN RESPONSE FACTOR gene family members in *Arabidopsis thaliana*: unique and overlapping functions of ARF7 and ARF19. *Plant Cell* **17**, 444–463 (2005).
16. Weijers, D. *et al.* Developmental specificity of auxin response by pairs of ARF and Aux/IAA transcriptional regulators. *EMBO J.* **24**, 1874–1885 (2005).
17. Ulmasov, T., Murfett, J., Hagen, G. & Guilfoyle, T.J. Aux/IAA proteins repress expression of reporter genes containing natural and highly active synthetic auxin response elements. *Plant Cell* **9**, 1963–1971 (1997).
18. Ramos, J.A., Zenser, N., Leyser, O. & Callis, J. Rapid degradation of auxin/indoleacetic acid proteins requires conserved amino acids of domain II and is proteasome dependent. *Plant Cell* **13**, 2349–2360 (2001).
19. Chapman, E.J. & Estelle, M. Mechanism of auxin-regulated gene expression in plants. *Annu. Rev. Genet.* **43**, 265–285 (2009).
20. Dreher, K.A., Brown, J., Saw, R.E. & Callis, J. The *Arabidopsis* Aux/IAA protein family has diversified in degradation and auxin responsiveness. *Plant Cell* **18**, 699–714 (2006).
21. Worley, C.K. *et al.* Degradation of Aux/IAA proteins is essential for normal auxin signalling. *Plant J.* **21**, 553–562 (2000).

22. Dharmasiri, N. *et al.* Plant development is regulated by a family of auxin receptor F box proteins. *Dev. Cell* **9**, 109–119 (2005).
23. Gray, W.M., Kepinski, S., Rouse, D., Leyser, O. & Estelle, M. Auxin regulates SCF[TIR1]-dependent degradation of AUX/IAA proteins. *Nature* **414**, 271–276 (2001).
24. Parry, G. *et al.* Complex regulation of the TIR1/AFB family of auxin receptors. *Proc. Natl. Acad. Sci. USA* **106**, 22540–22545 (2009).
25. Dharmasiri, N., Dharmasiri, S. & Estelle, M. The F-box protein TIR1 is an auxin receptor. *Nature* **435**, 441–445 (2005).
26. Kepinski, S. & Leyser, O. The *Arabidopsis* F-box protein TIR1 is an auxin receptor. *Nature* **435**, 446–451 (2005).
27. Calderón-Villalobos, L.I., Tan, X., Zheng, N. & Estelle, M. Auxin perception–structural insights. *Cold Spring Harb. Perspect. Biol.* **2**, a005546 (2010).
28. Tan, X. *et al.* Mechanism of auxin perception by the TIR1 ubiquitin ligase. *Nature* **446**, 640–645 (2007).
29. Greenham, K. *et al.* The AFB4 auxin receptor is a negative regulator of auxin signaling in seedlings. *Curr. Biol.* **21**, 520–525 (2011).
30. Vidal, E.A. *et al.* Nitrate-responsive miR393/AFB3 regulatory module controls root system architecture in *Arabidopsis thaliana*. *Proc. Natl. Acad. Sci. USA* **107**, 4477–4482 (2010).
31. Dharmasiri, N., Dharmasiri, S., Jones, A.M. & Estelle, M. Auxin action in a cell-free system. *Curr. Biol.* **13**, 1418–1422 (2003).
32. Timpte, C., Wilson, A.K. & Estelle, M. The axr2–1 mutation of *Arabidopsis thaliana* is a gain-of-function mutation that disrupts an early step in auxin response. *Genetics* **138**, 1239–1249 (1994).
33. Abel, S., Oeller, P.W. & Theologis, A. Early auxin-induced genes encode short-lived nuclear proteins. *Proc. Natl. Acad. Sci. USA* **91**, 326–330 (1994).
34. Prigge, M.J., Lavy, M., Ashton, N.W. & Estelle, M. *Physcomitrella patens* auxin-resistant mutants affect conserved elements of an auxin-signaling pathway. *Curr. Biol.* **20**, 1907–1912 (2010).
35. Vernoux, T. *et al.* The auxin signalling network translates dynamic input into robust patterning at the shoot apex. *Mol. Syst. Biol.* **7**, 508 (2011).
36. Alonso, J.M. *et al.* Five components of the ethylene-response pathway identified in a screen for weak ethylene-insensitive mutants in *Arabidopsis*. *Proc. Natl. Acad. Sci. USA* **100**, 2992–2997 (2003).
37. Ruegger, M. *et al.* The TIR protein of *Arabidopsis* function in auxin response and is related to human SKP2 and yeast Grr1p. *Genes Dev.* **12**, 198–207 (1998).
38. Hayashi, K. *et al.* Small-molecule agonists and antagonists of F-box protein-substrate interactions in auxin perception and signaling. *Proc. Natl. Acad. Sci. USA* **105**, 5632–5637 (2008).
39. Zhao, Y. & Hasenstein, K.H. Physiological interactions of antiauxins with auxin in roots. *J. Plant Physiol.* **167**, 879–884 (2010).
40. Hao, G.F. & Yang, G.F. The role of Phe82 and Phe351 in auxin-induced substrate perception by TIR1 ubiquitin ligase: a novel insight from molecular dynamics simulations. *PLoS ONE* **5**, e10742 (2010).
41. Walsh, T.A. *et al.* Mutations in an auxin receptor homolog AFB5 and in SGT1b confer resistance to synthetic picolinate auxins and not to 2,4-dichlorophenoxyacetic acid or indole-3-acetic acid in *Arabidopsis*. *Plant Physiol.* **142**, 542–552 (2006).
42. Prusty, R., Grisafi, P. & Fink, G.R. The plant hormone indoleacetic acid induces invasive growth in *Saccharomyces cerevisiae*. *Proc. Natl. Acad. Sci. USA* **101**, 4153–4157 (2004).
43. Nishimura, K., Fukagawa, T., Takisawa, H., Kakimoto, T. & Kanemaki, M. An auxin-based degron system for the rapid depletion of proteins in nonplant cells. *Nat. Methods* **6**, 917–922 (2009).
44. Evans, M.L., Ishikawa, H. & Estelle, M. Responses of *Arabidopsis* roots to auxin studied with high temporal resolution—comparison of wild-type and auxin-response mutants. *Planta* **194**, 215–222 (1994).
45. Jenik, P.D., Jurkuta, R.E. & Barton, M.K. Interactions between the cell cycle and embryonic patterning in *Arabidopsis* uncovered by a mutation in DNA polymerase epsilon. *Plant Cell* **17**, 3362–3377 (2005).
46. Prime, V. 2.1. (Schrödinger, LLC, 2010).
47. Laskowski, R.A., MacArthur, M.W., Moss, D.S. & Thornton, J.M. Procheck-A program to check the stereochemical quality of protein structures. *J. Appl. Crystallogr.* **26**, 283–291 (1993).
48. Sippl, M.J. Calculation of conformational ensembles from potentials of mean force. An approach to the knowledge-based prediction of local structures in globular proteins. *J. Mol. Biol.* **213**, 859–883 (1990).
49. Molecular Operating Environment 2008.10. (Chemical Computing Group Inc., 2009).
50. Korb, O., Monecke, P., Hessler, G., Stutzle, T. & Exner, T.E. pharmACOphore: multiple flexible ligand alignment based on ant colony optimization. *J. Chem. Inf. Model.* **50**, 1669–1681 (2010).

Author contributions
L.I.A.C.V. and M.E. prepared the manuscript. L.I.A.C.V. designed and performed the experiments and analyzed the data. X.T. and H.M. purified TIR1–ASK1 complex. L.I.A.C.V. expressed and purified AFB5–ASK1 complex. G.P. contributed to the generation of Y2H clones; C.D.O., A.I. and W.B. carried out homology modeling of AFB5 and docking experiments of picloram; and IAA. S.L., L.A., R.N. and S.K. expressed TIR1–ASK1 and AFB5–ASK1 constructs. S.L., S.K. and R.N. designed and performed SPR experiments. L.B.S. and N.Z. helped in the expression and purification of TIR1–ASK1 and AFB5–ASK1 complexes and the initial radioligand binding experiments. S.K., R.N., L.S. and N.Z. provided input to the manuscript. M.E. oversaw the project and approved the intellectual content.

Competing financial interests
The authors declare no competing financial interests.

Additional information
Supplementary information and chemical compound information is available online at http://www.nature.com/naturechemicalbiology/. Reprints and permissions information is available online at http://www.nature.com/reprints/index.html. Correspondence and requests for materials should be addressed to M.E.